ICRF Impurity Behavior with Boron Coated Molybdenum Tiles in Alcator C-Mod

S.J. Wukitch, M. Garrett, H. Barnard, B. LaBombard, Y. Lin, B. Lipschultz, E. Marmar, R. Ochoukov, M.L. Reinke, D.G. Whyte, G.H. Wright, and the Alcator C-Mod Team

MIT Plasma Science and Fusion Center, Cambridge MA 02139 USA

Email: wukitch@psfc.mit.edu

Abstract. Reducing impurity production associated with ion cyclotron range of frequency (ICRF) operation to an acceptable level in high confinement plasmas, particularly with metallic plasma facing components (PFC), requires an understanding of the underlying sources and associated physical mechanisms. To identify important impurity source locations, we have vacuum plasma sprayed ~100 μm of boron (B) onto a limited number of molybdenum (Mo) tiles. The boron coated tiles are located on the outer divertor shelf, plasma and RF outboard limiters. The inner wall, upper and lower divertor plates remained uncoated. In ICRF heated H-modes, the core molybdenum levels have been significantly reduced and remained at low levels for increased amount of injected RF energy. The core Mo level also no longer scales with RF power in L-mode. With boronization and impurity seeding (typically nitrogen or neon), the plasma performance was sustained for higher number of joules than without seeding. Impurity seeding also improved the ICRF antenna performance, suppressed antenna faults, without a significant increase in core Mo levels. Spectroscopic monitoring of the plasma limiter found that the impurity profile at the limiter was centered near the plasma mid-plane and the profile did not change shape with plasma current. From post campaign inspection, the B coating was not significantly eroded except in locations where melting occurred or where it peeled with little evidence of a discernable pattern. Trace material analysis found that the B surface was contaminated with Mo and tungsten (W). Although these observations are indirect in nature, these disparate observations suggest the impurity source associated with ICRF operation is more complicated than strictly sputtering due to enhanced RF sheaths.

1.0 Introduction

One of the primary challenges to utilization of ion cyclotron range of frequency (ICRF) as a heating, current drive or flow drive actuator is minimizing impurity production associated with ICRF operation. This situation becomes more difficult with metallic plasma facing components (PFC) and high confinement modes where even minor impurity sources can be intolerable. In next step devices including ITER, high-Z metallic PFCs and ICRF are being considered despite obvious obstacles.[1] Previously a prescription to ameliorate impurity production was developed empirically for experiments with carbon PFCs: boronization/berylliumization, aligned Faraday screen, and so called dipole antenna operation.[2] For ITER, beryllium has been proposed for some fraction of the PFC surfaces, including the ICRF Faraday screen. In C-Mod and many present experiments, boronization, an in-situ applied boron film, is utilized to control impurities but the coating has a limited effective lifetime. In C-Mod, the lifetime has been observed to be proportional to integrated RF Joules and the degradation is faster than in equivalent ohmic heated discharges suggesting the ICRF is enhancing the boron film erosion rate.[3, 4] The working assumption has been that sputtering due to enhanced RF sheaths is responsible for the increased erosion/impurity production.[5] Ample evidence from a number of experiments indicates that the ICRF is enhancing the sheath potential and the impurity sources track with the active antenna. Despite significant experimental effort, direct observation of the enhanced sheath potential and sputtering source at the same site and time has been lacking.

Although the geometric size of ITER (R=6.2m) is significantly larger than Alcator C-Mod (R=0.67 m), the C-Mod ICRF and plasmas have characteristics that are similar to expected ITER conditions. The C-Mod ICRF antennas power density is ~10 MW/m^2, in excess of the

expected ITER antenna power density. ICRF in C-Mod has strong single-pass absorption that results in toroidally localized RF fields. C-Mod utilizes high-Z (molybdenum) PFCs and the scrape off layer is also opaque to neutrals, an important consideration for impurity transport. In addition, beryllium has been proposed to cover most of the first wall and the ICRF faraday screen in ITER. In C-Mod, we can coat the PFCs with a low-Z boron film in-situ, using the so-called 'boronization' technique, or with vacuum plasma spray providing an opportunity to investigate the compatibility of high power ICRF and low-Z films. C-Mod also affords access to a wide variety of plasma conditions including edge localized modes (ELMs) and H-mode plasmas providing an opportunity to evaluate RF related impurity behavior over range of confinement modes.

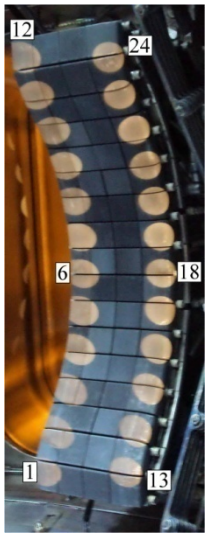

***Figure 1**: The main plasma limiter has 24 spectroscopic views of which 16 can be monitored simultaneously.*

Alcator C-Mod is a compact (major radius R = 0.67 m, minor radius a = 0.22 m), high field (BT ≤ 8.1 T) diverted tokamak[6]. The Alcator C-Mod discharges analyzed here are H-minority heated D discharge, D(H) (minority in parentheses), where the H cyclotron resonance is located near the magnetic axis. Although a range of toroidal fields and plasmas currents were investigated, the majority of the data was obtained for discharges with the on-axis toroidal field, B_T, was 5.4 T, and the plasma current, Ip, was 0.8-1 MA. Up to 5 MW of ICRF power is coupled to the plasma via three fast wave antennas. The two-strap antennas, D and E,[7] are operated in dipole (0,π) phasing, at 80.5 and 80 MHz, respectively and the four-strap antenna, J,[8] is operated at 78 MHz in dipole (0,π,0,π) and heating phase (0,π,π,0). In addition to standard plasma temperature and density diagnostics, core Mo content is monitored at Mo XXXI (11.6 nm) using a 2.2 meter grazing-incidence Rowland circle spectrometer. The local impurity line emission at the plasma limiter is monitored along 24 views as shown in *Figure 1*. The Mo I line and B I line are monitored at 386.4 nm and 419 nm respectively using an *f*/4, 0.25 m visible spectrometer. For a select number of molybdenum tiles, ~100 μm of boron has been vacuum plasma sprayed (VPS) onto the tiles. As shown in *Figure 2*, these tiles are on the outboard side of the tokamak on the outer divertor shelf, main plasma limiters, and the RF antennas. The VPS boron film is applied ex-situ in an argon atmosphere with the molybdenum tiles at an elevated temperature, ~600 °C.[9] The so-called boronization process utilizes an electron cyclotron resonance discharge (ECDC) in C-Mod to apply a thin film of boron on the PFCs. The boronization plasma characteristics have been reported elsewhere [10] and the boron deposition is limited to the radial region roughly bounded by the electron cyclotron resonance and the upper hybrid resonance. For the experiments described herein, a thin film (~200 nm) is applied prior to an experimental run day. Complicating the evaluation of the

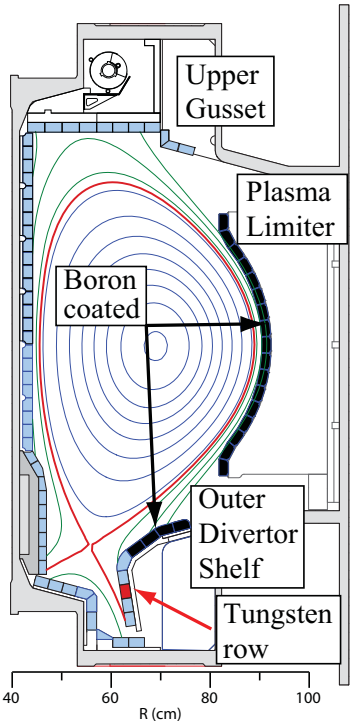

***Figure 2:** Boron coated tiles are located on the plasma limiter, RF limiters (not shown and at larger major radius than the plasma limiter), and outer divertor tiles.*

boron film is its degradation due to plasma operation prior to dedicated experiments designed to probe its impact on plasma performance.

For characterization of the VPS boron coating, visual inspection was performed both prior and post operation to monitor for spallation and melt damage. To monitor gross changes in coating thickness, an eddy current lift off technique measures the boron coating thickness and was performed in-situ. Simple visual inspection is also performed. For trace contaminants, ex-vessel proton induced x-ray emission (PIXE) is utilized. Briefly, PIXE uses a ~2 MeV proton beam to probe near surface atoms. Ionization leads to X-ray emission from the K and L shell electrons, which are used for identifying elements (Z > 20).[11]

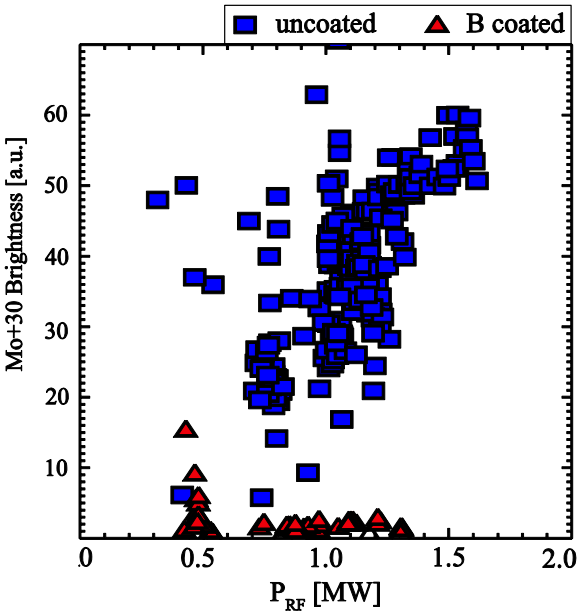

Figure 3: *Core Mo brightness independent of RF power with the B coated Mo tiles.*

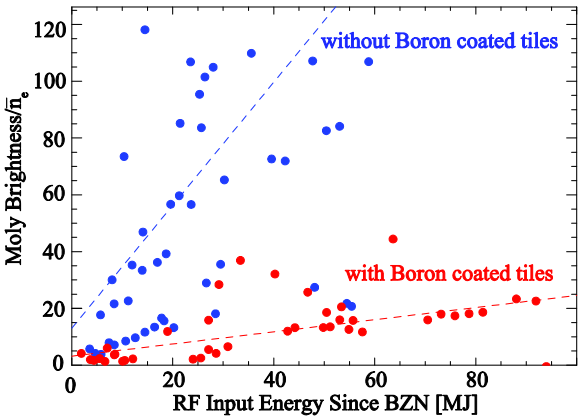

Figure 4: *Core Mo is significantly reduced and increases slower for integrated coupled RF joules for the B coated Mo case.*

2.0 Experimental Results

To investigate the impact the boron coating had on plasma performance and core molybdenum content, a series of L and H-mode discharges were run. For L-mode, upper single null discharges were utilized to raise the H-mode threshold (∇B away from the X-point) and the RF power was ramped from 0.1-1.5 MW. In these discharges, the core molybdenum levels no longer scaled with RF power, in contrast with previous results with boronization and molybdenum plasma facing components, see *Figure 3*.[3] For H-modes, a series of discharges were run following an overnight boronization to evaluate the core molybdenum content and rate of plasma performance degradation with injected RF energy. As shown in *Figure 4*, the core molybdenum levels were significantly reduced and remained at low levels for increased integrated RF Joules injected. As shown in *Figure 5*, the confinement was still reasonable after ~100 MJ of injected RF power, whereas without boron coated tiles the confinement had degraded at ~50 MJ of RF power.

In experiments to investigate compatibility of high radiative fraction and H-mode performance, nitrogen or neon impurity seeding of the H-mode improved the plasma and ICRF antenna performance. These experiments were performed after evidence the boron coating had been degraded due to melting of molybdenum tiles. A boronization was applied prior to the run and impurity seeding was used to radiate a high fraction of power and lower the power to the divertor.[12] Surprisingly, impurity seeding did not dramatically degrade the boronization lifetime or increase the core Mo levels. One may have expected the erosion rate to increase due to the increased sputtering arising from nitrogen or neon. Further seeding

experiments in H-mode showed that the plasma confinement was sustained for higher integrated RF energy if the seeding was utilized immediately following a boronization. These experiments also showed that as the impurity seeding level was reduced the core Mo radiation would increase. Impurity seeding also suppressed antenna faults due to arcs and injections from the antenna structure. A comparison of two discharges, shown in *Figure 6*, where one is seeded throughout the discharge (red) and the other (blue) is seeded until ~1.1 s, illustrates the improved antenna performance. Improved antenna performance from impurity seeding was most effective in H-mode discharges compared with L or I-mode discharges.

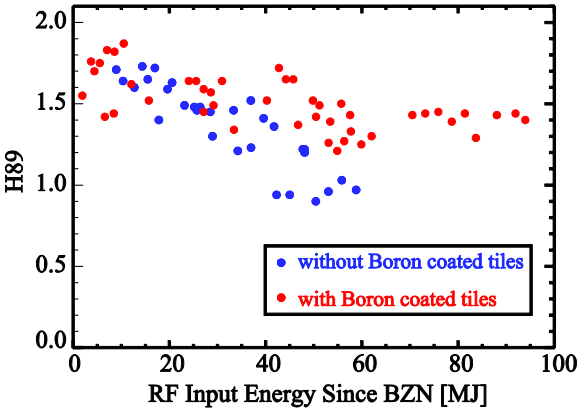

Figure 5: *Plasma performance as measured by plasma confinement is maintained for increased integrated injected RF Joules.*

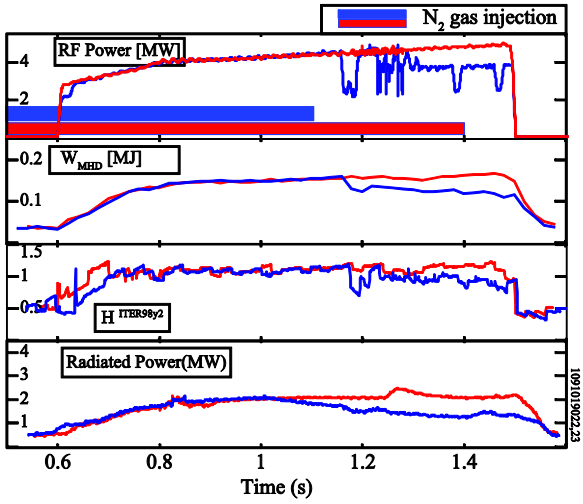

Figure 6: Antenna performance degrades when the impurity seeding is stopped at 1.1 s.

New spectroscopic views of the plasma limiter have been used to characterize the limiter molybdenum and boron source. This limiter is ~1 cm closer to the last closed flux surface than the RF antenna limiters and is magnetically connected to the 4 strap antenna (J antenna). As expected, the boron source dominates the molybdenum source for the VPS boron coated tiles on the limiter. The brightness profile is peaked at the plasma mid-plane where the plasma is closest to the limiter due to magnetic geometry. Although the limiter maps (is connected along the magnetic field) to the 4-strap antenna, the profile shape is unchanged with plasma q variation suggesting the impurity source profile shape is not dominated by sputtering from RF enhanced sheaths. From previous measurements, the enhanced sheaths were present at locations that mapped to the active antenna.[4] In H-mode, the maximum counts are weakly dependent upon the RF power; however, the impurity source is clearly enhanced in RF heated H-modes compared to Ohmic H-modes as shown in *Figure 7*.

Prior to operation the VPS boron coating thickness was measured in-situ by an eddy current technique. We used a Hocking Phasec2d and calibrated it against uncoated Mo tiles and known standards. The device allowed for average thickness of the coating to be found and the same technique was used following the campaign. Aside from the peeled boron location and where a limited number of molybdenum tiles were melted there was no discernable erosion of the boron film on any of the outer divertor shelf, plasma limiter, or RF protection tiles. The most severely melted molybdenum tiles are located at the midplane on two limiters. Additional melt damage was found on the leading and trailing edges of molybdenum tiles on the outer divertor shelf. The peeled tiles also did not show a discernable pattern: the neighbors of peeled tiles showed no signs of degradation or peeling in many cases. For comparison, an unexposed boron coated molybdenum tiles is shown in

Figure 8 and an example tile showing the coating degradation is shown in *Figure 9*. Note the tile to the right of the degraded tile is also coated and shows little visual evidence of degradation. Eddy current measurements confirmed that the boron film was not eroded.

To investigate surface contamination, we used the PIXE technique to probe for high Z impurities. Spectra for molybdenum, tungsten, stainless steel, and an unexposed, boron coated molybdenum were first analyzed to provide reference spectra for analysis of exposed boron coated tiles. As shown in *Figure 10*, the characteristic molybdenum spectrum has a strong peak near 3 keV and the tungsten spectrum has a pair of peaks from 9-12 keV. The stainless steel spectrum shows a number of peaks between 6-8 keV. The tiles were removed from the machine after the campaign but remained on their support module for the analysis. In *Figure 11* and *Figure 12*, the spectra from two representative exposed B coated tiles are shown. Both tiles have clear molybdenum contamination as evident by the clear peak at ~3 keV. In *Figure 12*, the tile spectrum also has significant W (peaks 9-12 keV) contamination in addition to clear molybdenum contamination. This level of contamination is more than an order of magnitude higher than previously measured on bare molybdenum tiles with the erosion dominated by sputtering.

3.0 Discussion

From an operational perspective, the boron coating was successful in reducing the molybdenum influx with ICRF operation. The coating however did not eliminate the need to boronize the machine. As found previously, the first in-situ boronization also reduces other high Z sources, particularly iron, for the remainder of the run period.[10] The VPS-coating quality needs to be improved through additional developmental work to prevent peeling and spalling observed on some tiles. The degradation is

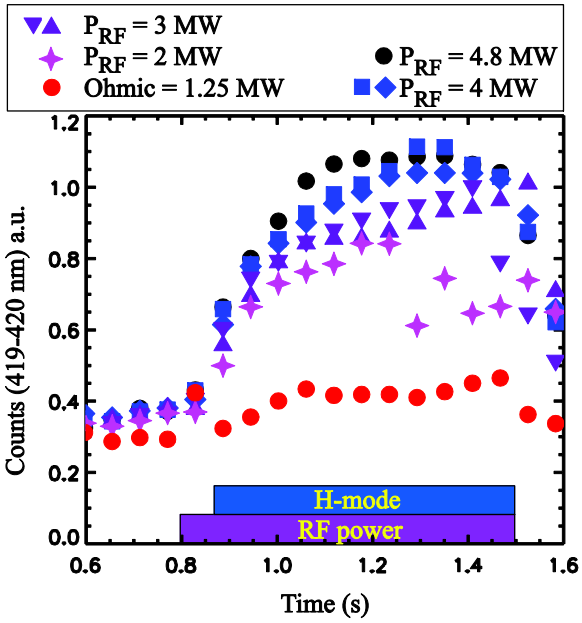

Figure 7: The impurity source at the limiter is enhanced for the RF heated versus ohmic H-mode and is weakly dependent on injected RF power.

Figure 8: Unexposed RF protection molybdenum tile coated with ~100 μm of boron. The boron film is porous and was approximately 50% theoretical density.

Figure 9: Example of the degradation of the boron film on molybdenum tiles on the outer divertor. Note the middle tile has degraded but the tile to the left and right are as installed.

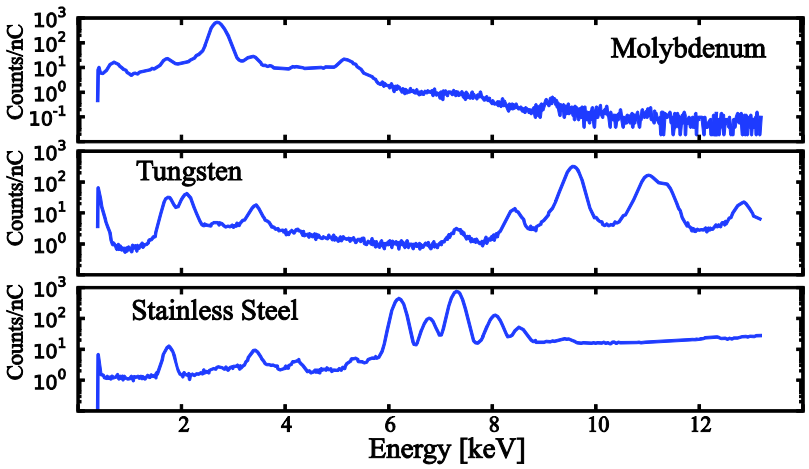

Figure 10: Molybdenum, tungsten, and stainless steel spectra measured by PIXE. The molybdenum spectrum has a distinct peak near 3 keV and tungsten spectrum has distinctive peaks between 9-12 keV. The stainless steel spectrum has a series of peaks between 6-8 keV.

likely due to poor film adhesion and thermal contact with the underlying Mo tile. The fundamental issues associated with boron coating are that the material has a high melting temperature (2300°C); is an insulator (difficult to heat directly); and has low mass (inhibits flow).

The lack of boron erosion is surprising and counter to our expectations. We estimated that the boron coating should have been eroded by 20-30 μm based on the 15-20 nm/s rates determined by earlier experiments.[13] We found no evidence of erosion with eddy current measurements with +/-5 μm. Furthermore, we expected an erosion pattern. If the erosion was to due to enhanced sheath voltages, we expected the corners of the antenna and objects that magnetically mapped to them to experience the highest erosion. Since there was no appreciable erosion, no pattern was found.

Another unexpected result is that plasma performance of impurity seeded discharges was maintained for integrated RF joules similar to unseeded discharges. Based on the enhanced sheath model, the addition of low Z impurities, nitrogen and neon, was expected to increase the sputtering rate and the boron erosion rate. Additionally, the Mo radiation was better controlled with increased seeding levels. These observations are indirect and interpreting the role of sputtering and other mechanism is highly speculative.

The observation that the impurity source profile at the plasma limiter is peaked on the plasma midplane is unanticipated. If RF enhanced sheaths were the underlying mechanism behind RF erosion and impurity production, one may expect the profile peaks to correspond to locations where RF sheaths are large – at locations connected to antenna corners. The impurity profile is peaked where the plasma has its closest approach to the limiter. Furthermore, the peak should have shifted with plasma current and it was unchanged.

Although these disparate observations are indirect in nature, they suggest the impurity source associated with ICRF operation in C-Mod is more complicated than strictly sputtering due to enhanced RF sheaths. These observations do not suggest that ICRF is not contributing to elevated impurity production. Indeed, the ICRF operation clearly increases the impurity source at the plasma limiter but not as expected from RF enhanced sheaths. Further with the

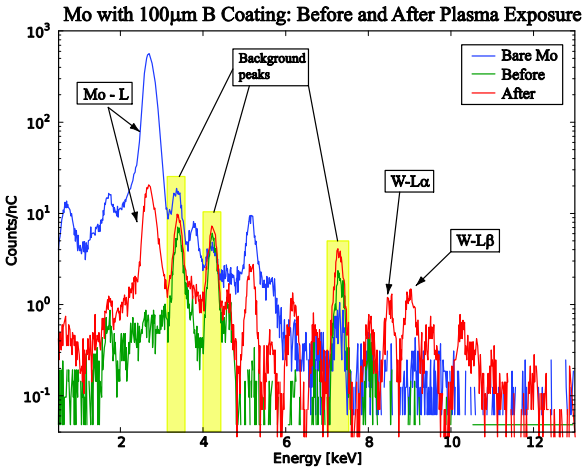

Figure 11: PIXE spectrum for an outer divertor tile after exposure to the plasma from the middle of a divertor module. The blue trace is a spectrum from solid molybdenum and the green trace shows a boron coated tile before exposure to the plasma. The red trace is the spectrum from an exposed boron tile.

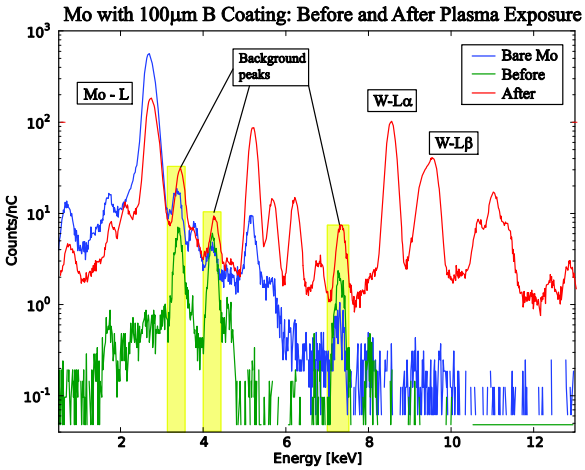

Figure 12: PIXE spectrum for an outer divertor tile after exposure to the plasma from the edge of a divertor module. The blue trace is a spectrum from solid molybdenum and the green trace is from an unexposured boron coated tile. The red trace is the spectrum from an exposed boron tile.

boron coated tiles, the molybdenum brightness is independent of ICRF power this suggests the primary core molybdenum sources are limited to these locations. The improved performance with impurity seeding and melted tiles suggest the ICRF impurity production could be a result of excessive thermal loads. Once the tiles melt, the situation further degrades and less ICRF power can be tolerated. A number of mechanisms could be possible including ICRF induced transport, localized edge power absorption, or fast ion losses that could contribute to enhanced thermal loads. Clear understanding of the mechanism or mechanisms is yet to be determined.

4.0 Acknowledgements

This work is support by Department of Energy Coop. Agreement DE-FC02-99ER54512.

Reference

[1] F. Najmabadi and the ARIES Team, Fusion Eng. and Design **80**, 3 (2006).
[2] J. Jacquinot et al., Fusion Eng Design **12**, 245 (1990).
[3] B. Lipschultz et al., Nuclear Fusion **41**, 585 (2001).
[4] S.J. Wukitch et al., J. Nucl. Mater. **363–365**, 491 (2007).
[5] J. Myra in 16th Top. Conf. on RF Power in Plasmas, AIP Conference Proceedings **787** (2006) 3 and J. Myra et al., Nuclear Fusion **46**, S455 (2006).
[6] I.H. Hutchinson, R. Boivin, F. Bombarda et al., Phys. Plasmas **1** (1994) 1511.
[7] Y. Takase et al., 14th Symp. on Fusion Eng., San Diego, 1992, (IEEE, Piscataway, NJ, 1992), p. 118.
[8] S.J. Wukitch et al., Plasma Phys. Control. Fusion **46**, (2004) 1479.
[9] S. O'Dell, private communication (www.plasmapros.com).
[10] B. Lipschultz et al., Phys. Plasmas **13**, 056117 (2006).
[11] H. Barnard et al., submitted to J. Nuclear Materials.
[12] J. Hughes et al., this conference EXC/P3-06.
[13] S.J. Wukitch et al., J. Nucl. Mater. **390-91**, 951-954 (2009).